The Journal of Engineering

The 9th International Conference on Power Electronics, Machines and Drives (PEMD 2018)

IET Journals
The Institution of Engineering and Technology

Design route towards a PM machine for rotorcraft environments

eISSN 2051-3305
Received on 21st June 2018
Accepted on 31st July 2018
E-First on 4th April 2019
doi: 10.1049/joe.2018.8070
www.ietdl.org

Dominic North[1] ✉, *Jason Yon*[1], *James Baker*[1], *Julian Booker*[1], *Phil Mellor*[1]

[1]*Electrical Energy Management Group (EEMG), University of Bristol, Bristol, UK*

✉ *E-mail: dn1847@bristol.ac.uk*

Abstract: This paper discusses the design route followed in the development of a permanent magnet (PM) machine for electrical power generation on board a rotorcraft (helicopter). The focus of the machine design is to optimise system power density, efficiency, and robustness – all of which are crucial considerations in aerospace applications. A matrix of designs was created consisting of two stators with different winding conductors – copper and aluminium – and three rotors, each using different containment sleeve materials. These include two semi-permeable metallic sleeves, which act to decrease the effective air gap. Combinations of the different materials will yield different system-level power densities and efficiencies. Here, all the designs are presented along with the initial test results for the baseline machine combination validating the design predictions.

1 Introduction

In common with fixed-wing aircraft, substantial efforts are being made within the rotorcraft sector to develop more electric aircraft (MEA), where mechanical and hydraulic systems are replaced with electrical implementations [1, 2, 3, 4]. This move promises a range of potential system benefits including lower maintenance costs, greater efficiency, enhanced reliability, and reduced fuel burn. This evolution leads to substantial increases in electrical demand, which will need to be met by additional on board generation capacity. In the rotorcraft sector, careful consideration of the harsh high-vibration environment is crucial in the design of these generators, particularly when powering safety-critical systems.

In designing a new machine type for on board generation (as opposed to incremental improvement of existing topologies), there exists an opportunity to challenge current practices. The motivation is the search for a combination of machine topology, active materials, and construction techniques optimised for the specific application. The question is whether new machine designs, which incorporate modern high-performance materials and are optimised with the use of modern design tools, can offer competitive specific outputs to the existing, mature, wound-field designs. Underpinning this is the need to achieve the high reliabilities demanded in the aerospace sector. In addition, the design of an aerospace power generation system should be approached holistically. Reduction in system mass and/or increase of system power density must be prioritised over the reduction of individual component masses.

This paper discusses the design of a prototype permanent magnet (PM) machine for electrical generation on board a rotorcraft. The design process features three variations of rotor containment material and two different winding materials.

2 Existing on board power generation

Rotorcraft electrical power generation currently uses multistage wound-field synchronous generators, often employing machines very similar, or identical to, those used in fixed wing applications [5]. However, rotorcraft applications expose this topology to an environment rich in vibrational frequencies for which it was not primarily intended. This could result in machine lifetime being shortened, a reduction in reliability or an increase in maintenance costs.

For any aerospace application, reliability is of paramount importance. The vibrational environment present on board a rotorcraft is very different to that of a fixed-wing aircraft. Different frequencies and magnitudes of vibration may affect the reliability of a given machine and make it suitable for one craft but not another. A particular concern, in the case of the conventional aerospace three-stage generator, is the reliability and lifespan of the rotating diode packs. These diodes rectify the supply from the main exciter stage to provide a DC field to the main generator stage. While they are designed to perform well under high centripetal loads and have a long service history in (relatively benign) fixed wing aircraft, these diode packs are complex mechanical assemblies. They would, therefore, be expected to have a reduced life when used in aggressive, high-vibration environments such as a rotorcraft and would incur maintenance, material, and time costs [6, 7]. Furthermore, losses due to the current in the field windings and the diodes on the rotor causes heating necessitating forced-oil cooling in most cases. This adds complexity due to the plant required for the coolant oil routing, pumping, and heat rejection. On top of this, efficiency is reduced, both due to hydrodynamic losses on the rotor in the air gap [8] and also due to the power take off required to operate the oil jets. Stator cooling is conventionally achieved by the same forced oil jets, incurring the same complexity and efficiency losses.

The designs presented here are all surface-mounted PM (SMPM) machines. This topology has very low total rotor loss in comparison with the wound field machine and forced oil cooling can, therefore, be removed from the rotor. Stator cooling can be achieved with an oil jacket incorporated into the machine case, creating a compact machine with no coolant ingress to the air gap.

3 Design route

The use case for this machine is on board a future more electric rotorcraft (MER), where considerable electrical generation is required to drive primary and auxiliary subsystems. The electrical demands exceed those of current aircraft, where hydraulic and mechanical systems provide the majority of power transfer and actuation. The machine was designed to be one of four identical on board generators – offering modularity and some redundancy [4, 9].

The machine design was directed by its industrial use case. From there, the process was driven by thorough electromagnetic and thermal modelling with the design space constrained by the hard limits imposed by the application. For instance, the maximum machine dimensions were limited by the existing installation footprint on a particular rotorcraft. Minimisation of system mass was the prime objective, subject to meeting the required power demands. The initial electrical design specifications are summarised in Table 1.

Table 1 Electrical specifications $_1$Max designed shaft speed. Max testing capability: 16,000 rpm

voltage (phase-neutral), Vrms	125
power (continuous), kVA	50
power (2 min overload), kVA	75
peak overload, P.U.	2
shaft speed (nom), rpm	12,000
shaft speed (max[1]), rpm	20,000
efficiency, %	>95

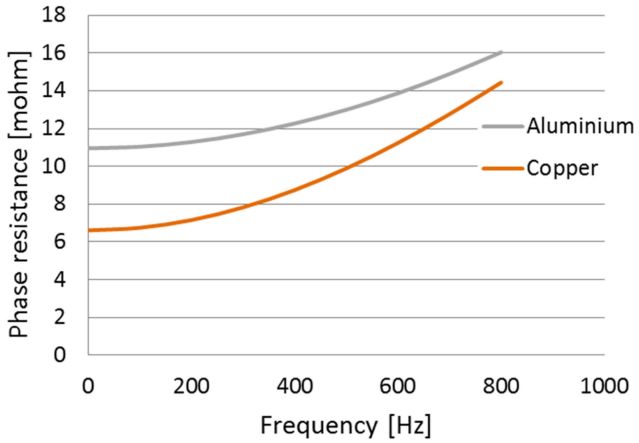

Fig. 1 *Copper and aluminium conductors: effective phase resistance (active) at 160C, with 3.0 mm × 4.3 mm conductors*

The machine was designed with three interchangeable rotors – each with a different magnetic containment material. This would allow comparison between the individual rotors, and their impact on the whole system performance. By designing to a common magnetic loading of 1.0 T and a common air gap diameter of 100 mm in all designs, the rotor and stator designs could be effectively decoupled. To enable experimental segregation of mechanical losses in the machine characterisation, a magnetically inert dummy rotor was also developed.

By decoupling the rotor and stator designs, an opportunity was also created to design for two different stator winding materials. In aerospace applications, the reduced mass and lower AC losses of aluminium are very attractive, as a possible alternative to copper. At higher frequencies, the relative differences in total losses between aluminium and copper windings become negligible as shown in Fig. 1. At this point, the mass savings of aluminium carry increasing benefit.

However, aluminium windings are a relatively immature technology and there are manufacturing and material concerns which must be addressed. These include fatigue from vibration and repeated operating cycles, manufacturing difficulties of the jointing process and concerns over joint longevity. However, should these be overcome, the system benefits are potentially great and make aluminium a worthy material for future development.

The containment materials and stator windings are discussed in Sections 3.2 and 3.3 and summarised in Table 2. The intent is to compare the different material combinations, to optimise the system benefits.

3.1 Materials and component selection

The priority in this design was to reduce system mass, partially through use of high performance materials and manufacturing methods. The stator was made from 0.1 mm CoFe laminations, offering high magnetic saturation of 2.35 T and low eddy current losses. A surface mounted PM design was chosen, due to its high efficiency and low complexity. The magnetic material was SmCo (Recoma 33E) offering a high 251 kJ/m^3 maximum energy product (BHmax).

Use of a Halbach array maximised the air gap magnetisation while minimising the back iron flux. This allowed the magnets to be directly mounted to the shaft without the need for a laminated back iron. This offered several machine-level benefits, including reduced material cost, less wastage and fewer interfaces, as well as reduced manufacturing complexity. Two of the three rotor shafts are shown in Fig. 2. The rotor shafts themselves were made from EN26T steel. The grade has relatively high strength and allows for a reasonable degree of structural optimisation and thus mass reduction.

Silicon nitride bearings were selected over conventional steel ones for a number of reasons. Ceramic rolling elements break any conductive path between rotor and stator and have a 60% lower density than steel. They, therefore, have lower inertia and better high-speed performance [10]. They also offer an extended service life due to reduced frictional heat generation and, their lower coefficient of thermal expansion delivers more consistent behaviour over a range of temperatures. All of these attributes are very beneficial to an aerospace system.

Table 2 Rotor and stator material combinations

Rotor			
containment	CFRP	15-5PH	304L
radial thickness, mm	1	0.5	0.5
assembly	filament wound	shrink-fit + machined back	shrink-fit
notes	baseline	semi-permeable	semi-permeable, laminated
stator			
winding material		copper	aluminium

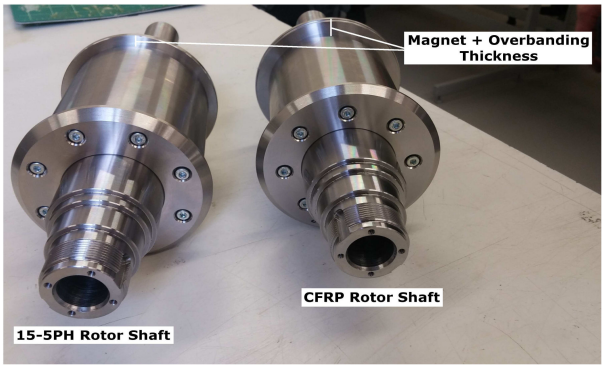

Fig. 2 *Rotor shafts for 15-5PH and CFRP containment methods, before construction of magnet arrays. The difference in magnet thickness due to containment permeability is clearly shown*

3.2 Rotor containment

Surface-mounted magnets require containment, especially at higher speeds. This project encompassed designs for three rotor containment materials. In aerospace PM machines, filament wound rotors are not conventionally used due to the possibility of damage during operation. Instead, PM containment tends to be implemented with nickel-chromium-based alloys, such as Inconel [11]. Being magnetically inert, these containment structures increase the effective air gap and so demand greater magnet mass beneath. Increasing the magnet mass demands an even greater containment thickness and so on. By using semi-permeable containment sleeves, the effective air gap can be reduced. For a given sleeve thickness, 304L has been shown to offer electromagnetic performance benefits over inert containments [11, 12]. In [13] (only available in Japanese text), preliminary analysis of a containment structure made of JIS SUS630 showed that this steel also resulted in a net improvement in air gap magnetisation. This grade of stainless steel (SS) is equivalent to AISI 17-4PH. The 15-5PH has a very similar chemical composition to 17-4PH and is, therefore, anticipated to give similar benefits.

The designed rotor containment materials were CFRP filament winding; a 15-5PH steel semi-permeable sleeve; and a 50% cold-

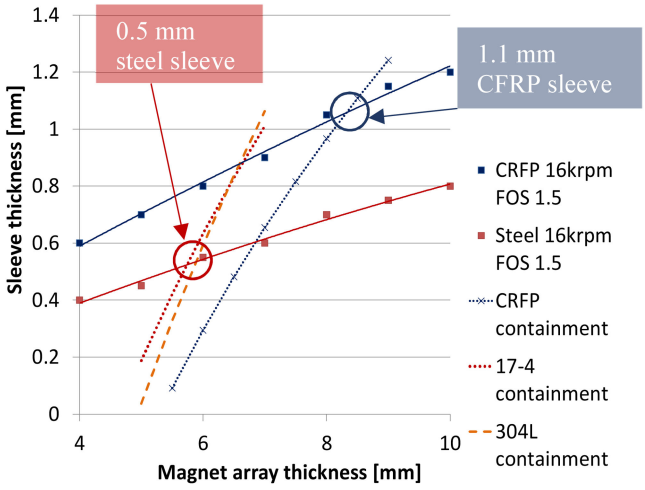

Fig. 3 *Optimising the magnet array thickness and containment thickness, to produce 1.0 T in the air gap*

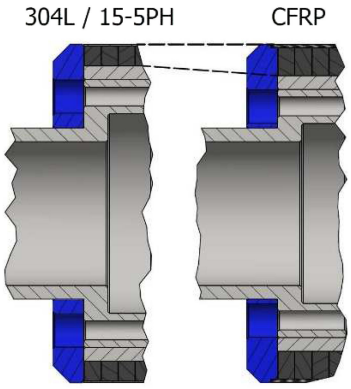

Fig. 4 *Comparison between magnet thicknesses for the semi-permeable and non-permeable containment types. Same rotor OD for both designs*

rolled 304L austenitic stainless steel laminated semi-permeable sleeve. These are summarised in Table 2.

FEA studies were undertaken to define the necessary magnetic volume to produce an air gap flux density of 1.0 T for each of the containment materials. The differences in their magnetic permeability demanded varying magnetic volume. This study was repeated for a range of containment thicknesses. In parallel, a stress analysis was conducted by Arnold Magnetics, to define the containment thickness needed to retain a given magnet mass at the machine's maximum speed. This was repeated for a range of magnet thicknesses and a factor of safety of 1.5 was applied.

The results of the two parallel studies were combined, thus the optimal combination of magnetic volume and containment thickness was defined. This is shown in Fig. 3.

From Fig. 3, the optimal combination can be read from the intersections of the two studies. The CFRP containment is necessarily thicker than the steel for a given magnet thickness, due to its lower mechanical strength. The CFRP also demands a greater thickness of magnet as it is magnetically inert. As a result, the CFRP design required a sleeve that was 1.1 mm thick and a PM array that was 8.2 mm thick. The semi-permeable sleeves offered better mechanical and magnetic performance. In these designs, a thinner containment of ~0.5 mm was needed to contain a 5.8-mm-thick PM array. Fig. 4 visualises this difference by comparing sections from the manufacturing drawings and Fig. 2 shows the manufactured rotor shafts for the CFRP and 15-5PH variants before population of the magnet arrays. In both figures, the difference in required magnet volume is clearly illustrated, with the inert containment requiring significantly more magnetic volume to produce the same air gap flux density.

Table 3 Electrical design specifications

poles	8
frequency, Hz	800
slots	48
conductors per slot	2
phases	3
slots/pole/phase	2
short pitch [slots]	1

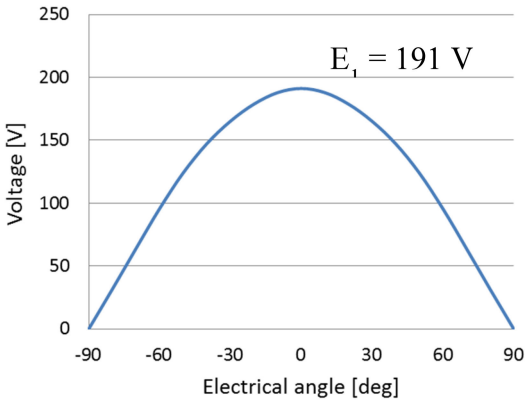

Fig. 5 *EMF waveform for the machine using 304L rotor containment*

3.3 Stator windings

Designs were made for both copper and aluminium wound rotors. Both designs were double-layer, with rectangular section conductors and hairpin style turns at one end. The wire gauges were slightly different, due to different stock available. The copper section was 4.30 mm × 3.0 mm, and the aluminium was 4.0 mm × 3.0 mm. Both were insulated with polyester/polyamide-imide coatings to IEC 60317-29 standard. The connection ends were crimped and soldered, with an internal star point formed. Beside the electromagnetics, this design offered practicality, with minimal external wiring. For the prototype machine (intended for characterisation and development), the connection ends would be brought out of the machine, where an external star point could be formed. This allowed flexibility in the testing programme, with easy arrangement of the windings for open-circuit, short-circuit, and DC tests.

3.4 Electromagnetic and thermal design

Electrical and electromagnetic design largely informed the physical machine characteristics and form factor. The initial dimensions and topology were defined using an analytical sizing tool, with numerical electromagnetic modelling used to optimise the design. This allowed rapid convergence to the bulk dimensions, followed with extra precision in the optimisation stages. The resulting design choices are summarised in Table 3. The design framework combined an FEA electromagnetic model, using FEMM [14], with electrical circuit models created in Simulink [15]. Further FEA was combined with a lumped parameter model for thermal considerations and verified using Motor-CAD [16]. The optimisation process was automated, with a parameterised script controlled in MATLAB [17].

The machine EMF and magnetic loading were given by open-circuit FEA and repeated for each rotor containment. Example waveforms are shown in Figs. 5 and 6, modelled on the semi-permeable 304L rotor containment.

Following a well-documented route to validation, tests were carried out on Motorette subassemblies to define the bulk thermal resistance network. Results were input to motor-CAD to verify the machine thermal model.

By omitting the oil jet cooling to rotor and stator, it was feasible to incorporate an integral oil jacket instead. Reasonable oil jacket performance could be assumed from other machines, lending confidence to this design's ability to achieve power density. The

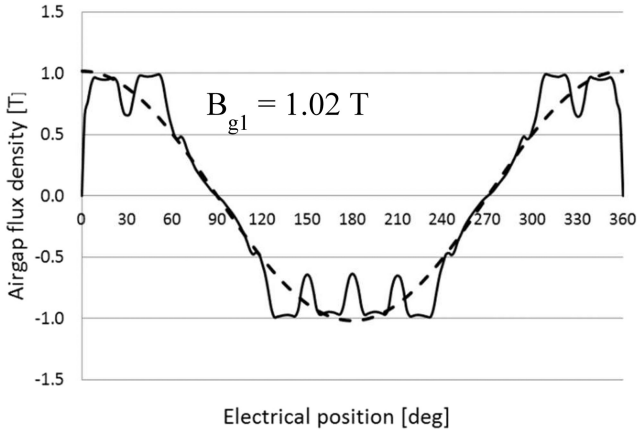

Fig. 6 *Magnetic loading for the machine using 304L rotor containment. The fundamental component of air gap flux density is 1.02 T*

Fig. 7 *Test rig apparatus before connections*

jacket's thermal effect was modelled in motor-CAD as a constant temperature element, forming the base point for the other machine temperatures. The necessary oil flow rate to achieve this constant temperature was returned.

4 Prototype development

At a manufacturing level, the copper wound stator was prioritised over the aluminium one. This decision took into account the conservatism shown towards aluminium at present and has allowed continuing small-scale studies on aluminium to be conducted in parallel. In this way, the three rotor variants will be initially benchmarked against a copper baseline. In the future, they will be compared again under an aluminium-wound stator, which will take advantage of any manufacturing advancements which have been made in parallel.

Upon completion of the aluminium wound stator, there will be six permutations of the machine for comparison. At the present time, a baseline machine has been constructed and assembled, using a copper-wound stator and CFRP rotor containment. This machine reflects the more 'standard' materials and will provide a basis of comparison for the more novel combinations. The 15-5PH contained rotor has also been fabricated and will be tested shortly. The 304L contained rotor has been manufactured and is awaiting final assembly and magnetisation of the Halbach array. The performance of the baseline machine has been validated and is described in Section 5.

The test apparatus for these machines is a four-quadrant induction machine dynamometer system. The prime mover is an Oswald QDI test rig motor with a rated power of 60 kW and a top speed of 16,000 rpm. The dynamometer is fitted with a high-precision HBM T12 torque transducer rated at 500 Nm. Data acquisition was conducted via a high-performance HBM GEN7tA platform which allowed electrical signals to be logged at high-resolution, and at up to 2 MS/s, synchronised with torque and speed data capture. An additional advantage of this platform is that its scalability offers the possibility to support system level tests incorporating other machines or aerospace electrical systems (Fig. 7).

Table 4 Preliminary test results

Parameter	Measured	Design	Variance, %
EMF at 12,000 rpm	188 Vpk	173 Vpk	+9
short circuit current	800 Arms	760 Arms	+5
phase resistance at 800 Hz	13 mΩ	14 mΩ	−6
phase inductance	33 μH	32 μH	+3

Notes: EMF and short circuit current measurements taken at room temperature, the design was for a hot rotor. The phase resistance was calculated from impedance measurements.

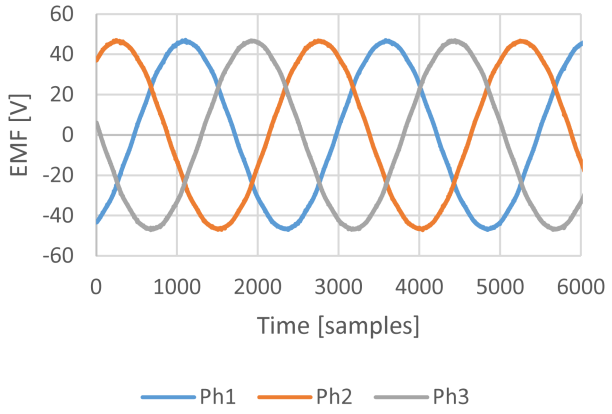

Fig. 8 *Example preliminary EMF for the CFRP rotor containment and copper-wound stator*

5 Initial test results

Initial results using the CFRP containment, in a copper-wound stator are presented in Table 4, against the designed values. The preliminary EMF waveform measured under test is shown in Fig. 8. It can be seen that the EMF is highly sinusoidal, with no significant harmonics. The measured EMF has a slightly higher fundamental component than the design predictions. This is because the design values incorporate the PM material's thermal coefficient of B_r and are presented for the machine's in-service temperature, whereas the measured values are taken at room temperature.

6 Conclusions and further work

It has been shown that a PM machine, with highly simplified architecture in comparison to a wound rotor machine, can provide significant power generation for running of electrical subsystems on board a MEA. The design work has yielded promising results regarding the use of semi-permeable containment, which will be verified under test in the near future.

Upon completion of testing for the three rotor variants, a comparative study will be able to assess the system benefit of each material. Upon completion of the aluminium-wound stator, further combinations will be available.

Pending the electromagnetic results on both stators, it is intended to further investigate the mechanical suitability of aluminium windings in a high-vibration environment, in particular, integrity and longevity of the jointing process. Possibilities include the use of ultrasonic soldering techniques, combined with more traditional mechanical jointing processes.

7 Acknowledgments

The authors would like to acknowledge the support of Leonardo Helicopters, Yeovil, UK. Particular thanks are extended to Dr Paul Brinson, Mr Martin Barber and Mr Keith Stickels for their invaluable technical input and ongoing support. The authors are

also very grateful to HBM UK ltd for the loan of a GENESIS eDrive data acquisition system, under their university support program.

8 References

[1] Sarlioglu, B., Morris, C. T.: 'More electric aircraft: review, challenges, and opportunities for commercial transport aircraft', *IEEE Trans. Transp. Electrification*, 2015, **1**, pp. 54–64

[2] Wheeler, P., Bozhko, S.: 'The more electric aircraft: technology and challenges', *IEEE Electrific. Mag.*, 2015, **2**, pp. 6–12

[3] Fabri, G., Parasiliti, F., Tursini, M., *et al.*: 'PM brushless motor for helicopters electric tail rotor drive system'. 2017 IEEE Int. Electric Machines and Drives Conf. (IEMDC), Miami, FL, USA, 2017

[4] Mellor, P. H., Yon, J., Baker, J. L., *et al.*: 'Electromagnetic and thermal coupling within a faulttolerant aircraft propulsion motor'. 2017 IEEE Int. Electric Machines and Drives Conf. (IEMDC), Miami, FL, USA, 2017

[5] Safran Electrical and Power: 'AC generation', 2017, [online]. Available at https://www.safran-electricalpower.com/electrical-systems/electrical-generationsystems/main-generation/c-variable-generation, accessed 19 January 2018

[6] Jing, T., Yang, C., Yang, Y., *et al.*: 'Simulation and fault detection for aircraft IDG system', *Procedia Eng.*, 2011, **15**, pp. 2533–2537

[7] Tang, X., Fan, D., Liu, L., *et al.*: 'Fault signal analysis for aircraft generator rectifier'. Proc. of the First Symp. on Aviation Maintenance and Management, Xi'an, China, 2014

[8] Sangha, P. S., Sawata, T., Yon, J., *et al.*: 'Assessment of fluid drag loss in a flooded rotor electrohydrostatic actuator motor'. 2015 IEEE Int. Electric Machines Drives Conf. (IEMDC), Coeur d'Alene, ID, USA, 2015

[9] Stickels, K., Brunetti, M. B., Barber, M., *et al.*: 'Advances in helicopter electric tail rotor drive'. Proc. of the European Rotorcraft Forum, Milan, Italy, 2017

[10] SKF Group: 'Hybrid bearings', February 2012, [online]. Available at http://www.skf.com/binary/68-48505/12507-EN-Hybrid-bearings.pdf., accessed 19 January 2018

[11] Yon, J. M., Mellor, P. H., Wrobel, R., *et al.*: 'A semi-permeable containment sleeve for highspeed PM machines'. 5th IET Int. Conf. on Power Electronics, Machines and Drives (PEMD 2010), Brighton, UK, 2010

[12] Yon, J. M., Mellor, P. H., Wrobel, R., *et al.*: 'Analysis of semipermeable containment sleeve technology for high-speed permanent magnet machines', *IEEE Trans. Energy Convers.*, 2012, **27**, pp. 646–653

[13] Sakai, K., Tokumasu, T., Itou, K.: 'Magnetic field analysis of a super-high-speed permanent magnet motor with a new rotor', *JSAEM*, 1996, **4**, pp. 40–45

[14] Meeker, D.: 'Finite element method magnetics', Finite, [online]. Available at www.femm.info/wiki/HomePage., accessed 19 January 2018

[15] MathWorks: 'Simulink', MathWorks, [online]. Available at https://uk.mathworks.com/products/simulink.html., accessed 19 January 2018

[16] Motor Design Ltd: 'Motor-CAD software', Motor Design Ltd, [online]. Available at https://www.motordesign.com/motor-cad-software, accessed 19 January 2018

[17] MathWorks: 'MATLAB', MathWorks, [online]. Available at https://uk.mathworks.com/products/matlab.html., accessed 19 January 2018